

Microhardness and structure of high pressure crystallized poly(ethylene terephthalate)

F. J. Baltá Calleja*

Instituto de Estructura de la Materia, CSIC, Serrano 119, 28006 Madrid, Spain

and O. Öhm and R. K. Bayer

Institut für Werkstofftechnik, Universität GH Kassel, Möncherbergstrasse 3, D-3500 Kassel, Germany

(Received 1 December 1993; revised 11 April 1994)

The microindentation hardness (H) of PET samples crystallized isothermally at various temperatures from the melt under high pressure (4 kbar) was determined in order to establish correlations with the thermal properties and microstructure. The results reveal that these materials show density, enthalpy of fusion, and melting temperature values which are close to those corresponding to chain extended crystals. The high crystallinities obtained ($\alpha=0.70\text{--}0.95$) for high pressure crystallized PET are shown to give rise to unprecedentedly high microhardness values, ranging between 300 and 400 MPa. The data are analysed on the basis of a two-phase model which allows an estimation of the influence of crystal thickness upon H . Finally, the temperature dependence of high pressure crystallized PET is also examined.

(Keywords: poly(ethylene terephthalate); microhardness; anabarc crystallization)

INTRODUCTION

The microhardness, H , of poly(ethylene terephthalate) (PET) crystallized at atmospheric pressure from the glassy state, with a wide range of structures, has been recently investigated¹. Two main types of morphologies were examined: (i) structures in which the growth of the spherulites was not completed, obtained by interrupting the primary crystallization, and (ii) structures in which spherulitic growth was completed. It was shown that in the former materials, H is a linear function of the volume fraction of the spherulites and depends on crystallization time and catalyst content. For the latter materials, H appeared to be almost independent of crystal thickness and crystallinity in the range of crystallization temperatures, T_A , between 120 and 240°C¹. In this temperature range, the crystal thickness, l_c , derived from small-angle X-ray scattering (SAXS), increases from 27 up to ~59 Å^{1,2}. This result is at variance with the dependence of H on the crystal thickness which has been observed for many polymers^{3,4}. Furthermore, it was shown that the constancy of H with T_A was consistent with the parallel constancy of the linear degree of crystallinity, i.e. $\alpha_L = l_c/L \sim 0.7$, measured over the same crystallization temperature interval, with L being the X-ray long period¹. The difference between α_L , as derived from SAXS, and the crystallinity value α , derived from the density, has been shown to be due to the existence of amorphous domains outside of the lamellar stacks which are larger than those within the stacks².

A two-step cold drawing process has been used to prepare highly oriented PET, containing crystals of high perfection, with superior mechanical properties⁵. In a recent study, we have shown that the injection moulding of high-molecular-weight PET, when using a mould that introduces elongational flow, can also give rise to crystalline oriented PET with enhanced mechanical properties⁶.

In order to investigate the correlation between the microhardness and the microstructure of PET samples with an even higher degree of crystallinity and larger crystal thickness values, in this present study we have prepared high-pressure PET samples which have been crystallized from the melt under different conditions. It is well known that the anabarc crystallization of polymers yields extended chain structures with enhanced thermal and mechanical properties⁷⁻¹¹. However, as far as we are aware, data concerning the anabarc crystallization of PET are still missing. Finally, we also wish to report the temperature dependence of the microhardness of these high pressure crystallized PET materials.

EXPERIMENTAL

Materials

PET samples of high crystallinity were prepared by using a hydraulic press. Amorphous PET pellets were melted in a cylindrical mould at a temperature of 275°C for 35 min. The molten pellets were then pressed under a pressure of 500 bar into the form of platelets (2 mm

*To whom correspondence should be addressed

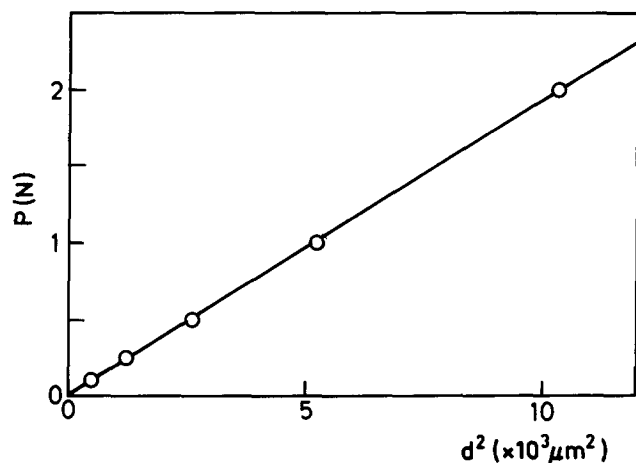


Figure 1 Plot of the load (P) against the square of the indentation diagonal for a PET sample crystallized under 4 kbar for 1 h at $T_A = 290^\circ\text{C}$

thick with a diameter of 20 mm). While maintaining this pressure, the temperature was reduced to 45°C . The pressure was then increased up to 4 kbar and the samples concurrently annealed at various temperatures, T_A , of 290, 300, 310, 315 and 320°C for periods, t_A , of 1, 2 and 3 h. The selected temperature was then decreased to 45°C over a period of 10 min, with the pressing force finally being reduced to zero. After cooling to room temperature, the specimens were examined by various techniques.

Techniques

Differential scanning calorimetry (d.s.c.) measurements were carried out by using a Mettler DSC 30 calorimeter in order to derive the degree of crystallinity and the melting temperature of the samples. The d.s.c. scans were performed over the temperature range $25\text{--}300^\circ\text{C}$, using a heating rate of $10^\circ\text{C min}^{-1}$.

The crystallinity was determined from the ratio of the heat of fusion measured for each sample to the corresponding heat of fusion for infinitely thick crystals, i.e. $\Delta h_f = 135\text{ J g}^{-1}$ (ref. 12). The density was measured at 20°C by using the flotation method. Three pieces of each sample were immersed twice in carbon tetrachloride (density = 1.594 g cm^{-3}). The accuracy of each measurement was estimated to be $\Delta\rho = \pm 0.001\text{ g cm}^{-3}$. From the density, the mass degree of crystallinity was estimated, assuming a value ρ_c for the density of the crystals of 1.490 g cm^{-3} and a value of ρ_a of 1.338 g cm^{-3} for the amorphous density¹³.

The degree of degradation of the polymer was qualitatively estimated by melt volume flow index (MVI) measurements, which were carried out at a temperature of 300°C under a load of 1.26 kg. The space-time scanning diagram was measured. The value of the MVI was calculated by using the equation, $MVI = 427 l^3(\text{cm}^3)/t(\text{s})$, where l and t are the displacement length and the displacement time of the piston, respectively, and 427 is a geometrical factor.

Microhardness was measured using a microhardness tester with a square-based pyramid indenter. The H value was derived from the diagonal length of the indentation by using the relationship, $H = 1.854 p/d^2$, where 1.854 is a geometrical factor, p is the applied force in N, and d is the diagonal length of the indentation in m. For each

value of H , at least 10 measurements of d were carried out, and the mean value was calculated. Typically, loads of 0.15, 0.25 and 0.50 N were employed. Figure 1 shows, as an example, the linear dependence of the applied force on the squared diagonal length of indentation for a PET sample which had been crystallized under 4 kbar at 290°C for 1 h. A loading cycle of 6 s was used. The microhardness of the samples, derived from the slope of the p versus d^2 plots, was measured at room temperature. The temperature dependence of the microhardness was also examined for one selected sample ($T_A = 320^\circ\text{C}$, $t_A = 3$ h) over the range from room temperature up to 220°C using a hot-stage with a heat controller¹⁴. The surface temperatures of the samples were calibrated with organic compounds of known melting points. In order to obtain a suitable optical contrast of the impressions, a 100 \AA layer of Au/Pd alloy was evaporated onto the sample surface.

RESULTS

Table 1 shows the influence of the temperature and time of crystallization, when using a pressure of 4 kbar, on the values of the density, the enthalpy of fusion, the corresponding mass-average degree of crystallinity, the temperature of the melting peak and the microhardness. From the data of Table 1, we can immediately observe the extremely high values of the crystallinities, which range between ~ 0.5 and almost 1.0 for samples crystallized at this pressure. It is convenient to recall that in the case of PET samples crystallized at atmospheric pressure, the crystallinity varies, depending on the crystallization temperature, between 0.2 and 0.5². Figure 2 illustrates a typical d.s.c. scan for one of the PET samples that had been crystallized at $T_A = 290^\circ\text{C}$ for 1 h, plus that of another sample crystallized at $T_A = 320^\circ\text{C}$ for 3 h. It can be seen that the influence of increasing the temperature and time of crystallization clearly gives rise to a higher and sharper melting peak, suggesting the occurrence of much thicker crystals with a narrower distribution of crystal thicknesses. Table 1 additionally shows the good correspondence between the α_ρ and α_{DSC} values. Of great interest is the plot of the enthalpy of fusion as a function of density (Figure 3), which

Table 1 Density, crystallinity values derived from both density and from d.s.c., enthalpy of fusion, melting temperature and microhardness values of PET samples crystallized under a pressure of 4 kbar at various temperatures for different periods of time (see text for details)

T_A ($^\circ\text{C}$)	t_A (h)	ρ (g/cm^{-3})	α_ρ	α_{DSC}	ΔH (J g^{-1})	T_M ($^\circ\text{C}$)	H (MPa)
290	1	1.409	0.454	0.545	61.3	253.4	250
295	1	1.445	0.727	0.738	99.6	265.4	288
300	1	1.462	0.834	0.804	108.6	262.9	—
315	1	1.452	0.767	0.724	77.7	262.7	311
315	1	1.460	0.816	0.771	104.1	261.1	205
310	2	1.467	0.859	0.875	118.1	274.2	348
310	2	1.470	0.879	0.817	110.3	270.9	311
320	2	1.472	0.888	0.953	128.7	275.7	357
310	3	1.473	0.898	0.880	118.8	274.0	359
320	3	1.501	1.000	0.993	134.1	277.9	353
320	3	1.485	0.967	0.944	127	283.7	375
320	3	1.482	0.947	0.914	124	273.3	378
320	3	1.478	0.921	0.858	121	275.3	386

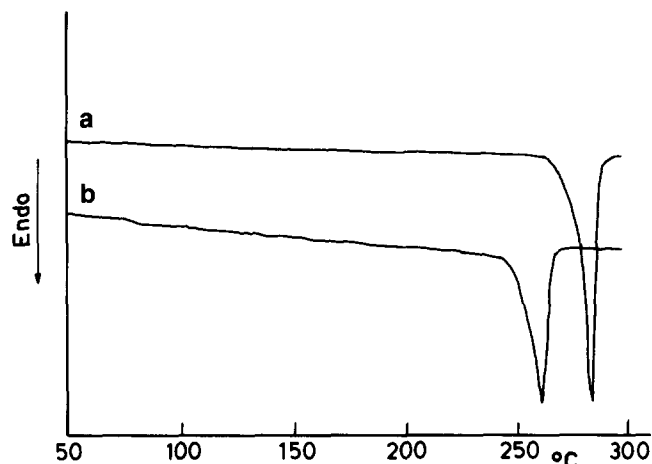


Figure 2 D.s.c. scans obtained for two PET samples crystallized from the melt at 4 kbar: (a) $T_A = 320^\circ\text{C}$ for 3 h; (b) $T_A = 250^\circ\text{C}$ for 1 h

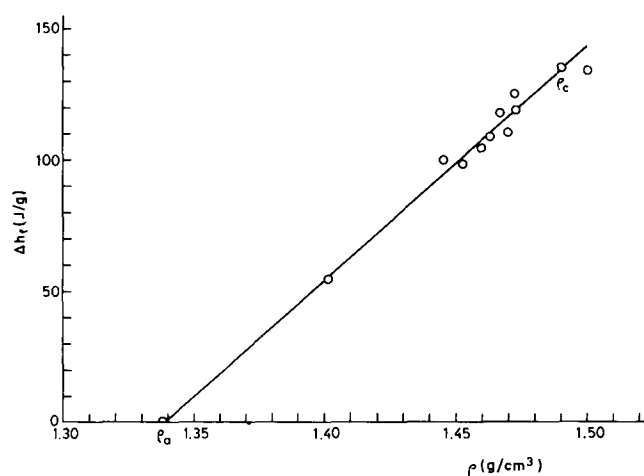


Figure 3 Plot of enthalpy of fusion as a function of density for the PET samples crystallized from the melt at 4 kbar

extrapolates for $\Delta h_f = \Delta h_f^\infty (135 \text{ J g}^{-1})^{13}$ to $\rho \sim 1.49 \text{ g cm}^{-3}$, a result which is very close to the value of $\rho_c = 1.4895 \text{ g cm}^{-3}$, proposed by Gehrke and Zachmann¹³. Furthermore, this plot shows an extrapolation for $\Delta h_f = 0$ to a ρ value of 1.338 g cm^{-3} , which also agrees well with the result given by the above mentioned authors¹³ for the density of the fully amorphous polymer. In addition, the data of Figure 3 highlight the fact that high pressure crystallized PET materials exhibit values of ρ and Δh_f which are much higher than those normally obtained for PET samples crystallized at atmospheric pressure. For example, for conventional PET samples having a degree of crystallinity of 0.3, $\Delta h_f = 35 \text{ J g}^{-1}$ and $\rho = 1.378 \text{ g cm}^{-3}$ (refs 1, 13).

Although at atmospheric pressure the T_m of an extended chain crystal of a polymer is 2–3 K lower than T_m° ¹⁵, the T_m values obtained for PET (shown in Table 1) indicate melting temperatures which should be close to the equilibrium melting temperature of PET. The plot of $1/T_m$ against α_{DSC} (illustrated in Figure 4) allows us to draw an extrapolation of $1/T_m$ for $\alpha = 1$, which gives an approximate value for the equilibrium melting temperature of PET (infinitely thick crystals) of $T_m^\circ = 285^\circ\text{C}$.

The high crystallinities obtained for these PET high pressure crystallized samples give rise to unprecedentedly high microhardness values, ranging from 300 to $\sim 400 \text{ MPa}$. No evidence for any anisotropy of the resulting indentation in the high pressure crystallized PET samples was obtained. Table 1 shows the very noticeable increase of H with increasing crystallinity.

Measurements of the MVI for these PET samples show a considerable increase from a value of 174 cm^3 per 10 min displacement time for the initial pellets, up to $\sim 1700 \text{ cm}^3$ per 10 min displacement time for the high pressure crystallized samples. This increase in the MVI suggests a substantial decrease in the molecular weight, as confirmed independently by viscosity measurements ($M_w = 30\,000$ for the initial pellets, and $M_w \sim 8000$ for the high pressure crystallized sample at $T_A \sim 289^\circ\text{C}$).

DISCUSSION

In PET samples crystallized at atmospheric pressure, the degree of crystallinity typically varies between 0.2 and 0.5². However, the linear crystallinity derived from SAXS measurements (α_L) was found to be $\sim 0.7^2$. This discrepancy between the α and α_L values has been explained by the presence of amorphous regions which are lying irregularly between the semicrystalline lamellae stacks². These interstack amorphous regions are, in fact, the first ones to be attacked and removed during the initial stage of hydrolysis in water at elevated temperatures¹⁶. The occurrence of a fibre texture in polymers has been associated with the presence of a clear anisotropy in the indentation pattern^{7,17}. Thus, the lack of any indentation anisotropy on the surface of our high pressure crystallized PET samples suggests that the materials are mechanically isotropic. The study of the microstructure of these samples by diffraction techniques will be the subject of a separate forthcoming study.

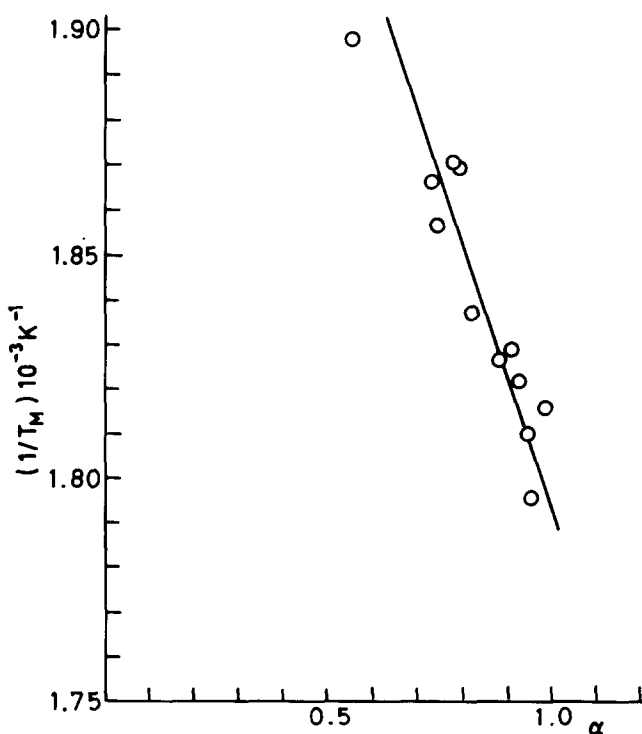


Figure 4 Plot of $1/T_m$ versus α_{DSC} for the PET samples crystallized from the melt at 4 kbar

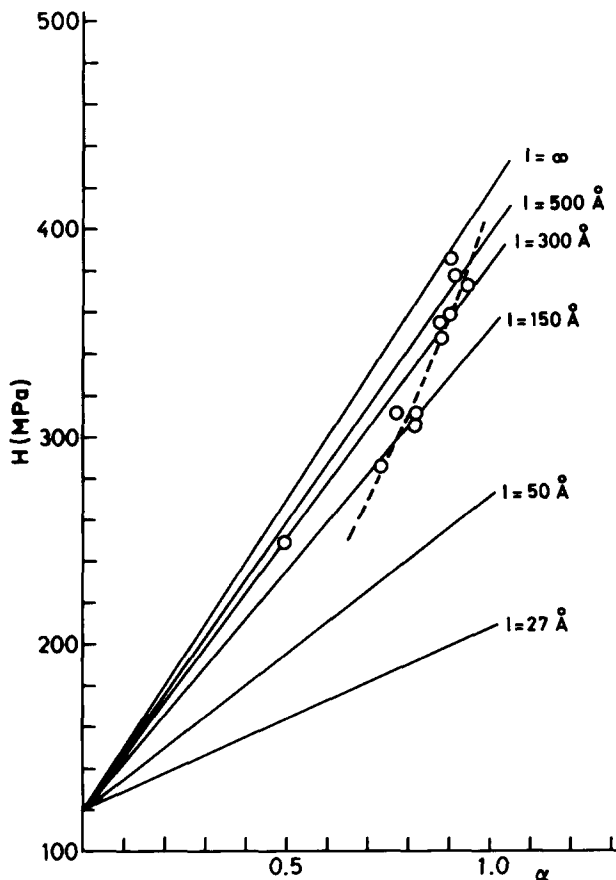


Figure 5 Variation of microhardness of high pressure crystallized PET with increasing crystallinity (α_{DSC}): experimental data (open symbols); calculated data from equation (2) (solid lines) are given for the l_c values, assuming $b = 28 \text{ \AA}$

Except for the sample crystallized under high pressure at the lowest temperature, i.e. $T_A = 290^\circ\text{C}$, the rest of the high pressure crystallized samples examined in this study show macroscopic crystallinities higher than 0.7. The high crystallinity values that were obtained suggest that these high pressure crystallized materials exhibit a new structure in which the lamellae stacks are no longer separated by large amorphous regions of irregular size^{1,2}.

If we assume a two-phase model, the hardness of such a system is given by the following expression³:

$$H = H_c \alpha + H_a (1 - \alpha) \quad (1)$$

where H_c and H_a are the hardness values for the crystalline and amorphous regions, respectively, and α is the macroscopic crystallinity, which in this present case should coincide with α_L . From ref. 1, H_a can be taken to be approximately equal to 120 MPa. The dependence of H_c upon the crystal thickness l_c , if one assumes a heterogeneous plastic deformation of the crystals under the indenter, has been shown to be of the following type⁴:

$$H_c = \frac{H_c^\infty}{1 + \frac{b}{l_c}} \quad (2)$$

where H_c^∞ is the hardness for an infinite crystal and b is a parameter which is related to the surface free energy σ_c of the crystals and to the energy Δh required for plastic deformation of the crystal through the formation of a

very large number of shearing planes. This b parameter is equal to $2\sigma/\Delta h$. The value of H_c^∞ can be estimated, for extended chain crystals, by extrapolation of the H data to $\alpha = 1$. From the data of Table 1, a value for 'infinitely thick' PET crystals of $H_c^\infty = 418 \text{ MPa}$ can be inferred. This value is somewhat higher than the H_c^∞ value previously proposed¹.

The above results emphasize the substantial reduction in chain length of the PET after anabarc crystallization (from $M_w = 30\,000$ to $8\,000$) suggesting the occurrence of crystal structures containing mainly chain ends, chain folds and only a few interlamellar connections at the crystal surfaces, i.e. with an absence of chain entanglements. Consequently we may assume that the b parameter, which is proportional to the surface free energy of the lamellae, remains nearly constant for these high pressure crystallized samples.

If we take $b = 28 \text{ \AA}$, which is the value obtained for the samples crystallized at atmospheric pressure with the highest crystallinity, then we can derive the l_c values from equation (2). By using now equations (1) and (2), together with $H_c^\infty = 418 \text{ MPa}$ and $b = 28$, we have drawn in Figure 5 a set of mastercurves, describing the double dependency of H upon α and l_c . The experimental microhardness data for the high pressure crystallized PET samples are also shown in Figure 5 for comparison.

The results suggest that, with increasing temperature and time of crystallization, the thickness of the crystals increases, giving rise to the observed rise in hardness with increasing α . It is to be noted that the dotted line is drawn from $\alpha = 0.7$ to almost 1, because it is mainly in this crystallinity range that the two-phase model is expected to be valid. For lower crystallinities, more complex structures have been observed^{1,8} and deviations from the two-phase model occur².

The expected dependence of H on l_c is confirmed by the experimentally obtained dependence of T_M (proportional to l_c) upon α , depicted in Figure 4. From Figure 5, we see that the highest crystallinity samples ($\alpha_{DSC} \sim 0.95$) imply crystal thicknesses contained within the range between 300 \AA and the fully extended chain length (with $M_w = 8\,000$, the chain length is $\sim 600 \text{ \AA}$).

In order to characterize the thermal stability of these very hard PET materials, we have investigated the temperature dependence of the microhardness for one of the PET samples with high crystallinity. The decrease of H with temperature is shown in Figure 6. The microhardness decrease for a sample of high pressure crystallized PET follows the exponential law:

$$H = H_0 \exp[-\beta(T - T_0)] \quad (3)$$

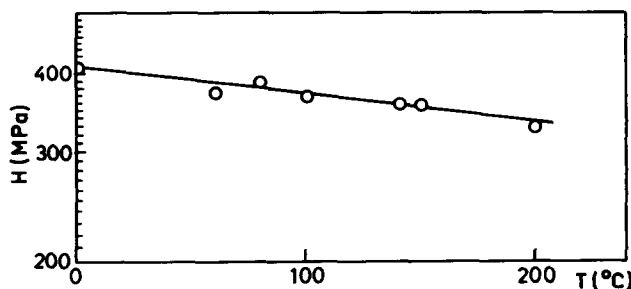


Figure 6 Log H as a function of temperature for isothermally crystallized PET ($T_A = 386^\circ\text{C}$) at 4 kbar

where T is the temperature, β is the coefficient of thermal softening and H_0 is the hardness at a given reference temperature T_0 . From the plot of *Figure 6*, we derive a value of $\beta = 1.16 \times 10^{-3} \text{ K}^{-1}$. It has been pointed out that deformation under compression of chain extended polymer crystals is dominated by a chain slip mechanism³. The fact that the high pressure crystallized material is primarily built up of chain extended crystals is supported by the results obtained for the β coefficient, which is constant below and above $T_g \sim 70^\circ\text{C}$. Such a relatively low rate of hardness decrease over such a wide temperature range (20–220°C) is unusual for a common polymer and indicates that high pressure crystallized PET shows a mechanical behaviour which is typical of a high performance material, such as that exhibited by metals¹⁹.

CONCLUSIONS

The main conclusions to be drawn from this work are as follows:

(1) Anabaric crystallization of PET (at 4 kbar) yields a class of high crystallinity materials with enhanced yield mechanical properties ($H \sim 400 \text{ MPa}$) and a relatively low thermal softening coefficient.

(2) Analysis of the microhardness data on the basis of thermodynamic predictions allows one to explain the high crystallinities of high pressure crystallized PET in terms of a two-phase model which yields relatively large crystal sizes.

(3) This microstructure gives rise to values of density, enthalpy and temperature of fusion, which are close to those expected for infinitely thick crystals.

ACKNOWLEDGEMENTS

Grateful acknowledgement is due to Comision Interministerial de Ciencia y Tecnologia (CICYT), Spain

(Grant 740/94E) for the generous support of this investigation. We are grateful to Professor H. G. Zachmann, University of Hamburg, for molecular weight determinations of the PET samples described in the text.

REFERENCES

- 1 Santa Cruz, C., Baltá Calleja, F. J., Zachmann, H. G., Stribeck, N. and Asano, T. *J. Polym. Sci. Polym. Phys. Edn* 1991, **29**, 819
- 2 Santa Cruz, C., Stribeck, N., Zachmann, H. G. and Baltá Calleja, F. J. *Macromolecules* 1991, **24**, 5980
- 3 Baltá Calleja, F. J. *Adv. Polym. Sci.* 1985, **66**, 117
- 4 Baltá Calleja, F. J. and Kilian, H. G. *Colloid Polym. Sci.* 1988, **266**, 29
- 5 Fakirov, S. and Evstatiev, M. *Polymer* 1990, **31**, 431
- 6 Rueda, D. R., Kubera, L., Baltá Calleja, F. J. and Bayer, R. K. *J. Mater. Sci. Lett.* 1993, **12**, 1140
- 7 Baltá Calleja, F. J. and Bassett, D. C. *J. Polym. Sci. (C)* 1977, **58**, 157
- 8 Wunderlich, B. 'Macromolecular Physics', Vol. 1, Academic, Cambridge, 1993, p. 217
- 9 Bassett, D. C. 'Principles of Polymer Morphology', Cambridge University Press, Cambridge, 1981, p. 167
- 10 Gogolewski, S. and Pennings, A. *J. Polymer* 1967, **18**, 647
- 11 Hirte, R., Schaper, A. and Schulz, E. 14th Europhysics Conference on Macromolecular Physics, Vilafranca del Penedes, September, 1982, Conference Abstracts. Vol. 6G, p. 58
- 12 Blundell, D. J. and Osborn, D. N. *Polymer* 1983, **24**, 953
- 13 Gehrke, R. and Zachmann, H. G. *Makromol. Chem.* 1981, **182**, 627
- 14 Baltá Calleja, F. J., Santa Cruz, C. and Asano, T. *J. Polym. Sci. Polym. Phys. Edn.* 1993, **31**, 557
- 15 Prime, R. B. and Wunderlich, B. *J. Polym. Sci. (A-2)* 1969, **7**, 2073
- 16 Cagiao, M. E., Baltá Calleja, F. J., Vanderdonckt, C. and Zachmann, H. G. *Polymer* 1993, **34**, 2024
- 17 Rueda, D. R., Bayer, R. K., Baltá Calleja, F. J. and Zachmann, H. G. *J. Macromol. Sci. Phys.* 1989, **28**, 265
- 18 Groeninckx, G. and Reynaers, H. *J. Polym. Sci. Polym. Phys. Edn* 1980, **18**, 1325
- 19 O'Neill, H. 'Hardness Measurements of Metals and Alloys', 2nd Edn, Chapman and Hall, London, 1967, p. 165